PAPER *Special Issue on Innovation in Antennas and Propagation for Expanding Radio Systems*

Performance Analysis of Subband Arrays*

Yimin ZHANG[†], ***Regular Member***, **Kehu YANG**[††], **Moeness G. AMIN**[†], ***Nonmembers***, ***and*** **Yoshio KARASAWA**[†††], ***Regular Member***

SUMMARY Several subband array methods have been proposed as useful means to perform joint spatio-temporal equalization in digital mobile communications. These methods can be applied to mitigate problems caused by the inter-symbol interference (ISI) and co-channel interference (CCI). The subband array methods proposed so far can be classified into two major schemes: (1) a centralized feedback scheme and (2) a localized feedback scheme. In this paper, we propose subband arrays with partial feedback scheme, which generalize the above two feedback schemes. The main contribution of this paper is to derive the steady-state mean square error (MSE) performance of subband arrays implementing these three different feedback schemes. Unlike the centralized feedback scheme which can be designed to provide the optimum equalization performance, the subband arrays with localized and partial feedback schemes are in general suboptimal. The performance of these two suboptimal feedback schemes depends on the channel characteristics, the filter banks employed, and the number of subbands.

key words: *subband array, space-time adaptive processing, adaptive array, multirate signal processing, mobile communications*

1. Introduction

Mobile communication systems are developing toward higher-speed digital wireless networks. Their applications are rapidly expanding from voice transmission to a wide class of multimedia information. In the new wireless networks, the communication channels are often frequency-selective, which makes the inter-symbol interference (ISI) to be highly pronounced. Another important problem in mobile communication is the co-channel interference (CCI), which is the result of frequency reuse in cellular systems.

Manuscript received December 15, 2000.

Manuscript revised March 15, 2001.

[†]The authors are with the Department of Electrical and Computer Engineering, Villanova University, Villanova, PA 19085, USA.

[††]The author is with ATR Adaptive Communications Research Laboratories, Kyoto-fu, 619-0288 Japan.

[†††]The author is with the Department of Electronic Engineering, University of Electro-Communications, Chofu-shi, 182-8585 Japan.

*This paper was presented in part at the International Symposium on Antennas and Propagation, Fukuoka, Japan, August 2000. The work of Y. Zhang is continued from his previous work when he was with the ATR Adaptive Communications Research Laboratories. The work of M.G. Amin is supported by the Office of Naval Research under Grant N00014-98-1-0176.

Adaptive arrays implementing spatial or spatio-temporal equalizations prove useful in suppressing both ISI and CCI, leading to improved communication quality and increased communication capacity [1]–[4]. Specifically, space-time adaptive processing (STAP) techniques are power tools to achieve spatio-temporal equalizations. The high complexity and slow convergence, however, are key issues in practical implementation of STAP systems.

Recently, subband adaptive array methods have been proposed as alternative tools for spatio-temporal equalization. The authors have proposed in [5]–[8] to use subband arrays to realize joint spatio-temporal equalizations. This concept has also been extended to subband STAP schemes [9], [10]. Compared with conventional STAP systems, subband adaptive arrays offer amenability to parallel implementations [8], rapid convergence [11], [12], and a reduction of processing complexity [13], [14]. Subband processing is cast in [15] as an elegant and computationally efficient solution to the needs for increased bandwidth in array processing applications.

The subband array methods proposed so far can be classified, in terms of the definition of error signals used to control the weight updation, into two major classes: (1) a centralized feedback scheme and (2) a localized feedback scheme. A subband array with the localized feedback scheme allows parallel subband processing with greatly reduced computations at each subband, accompanied with improved convergence. These features are vert attractive in STAP implementations, as the system complexity increases sharply when either or all of the data rate, delay profile, and the number of array sensors increase.

We propose in this paper the partial feedback scheme, which generalizes the above two feedback schemes. The proposed partial feedback scheme permits more flexibility in trading-off the system complexity, convergence, and the steady-state mean square error (MSE) performance.

Our main contribution in this paper is analysis of the MSE performance of subband arrays with the three different feedback schemes. For simplicity of analysis and comparison, it is assumed that the reference signal is available. For the centralized feedback schemes, reference [16] has shown that frequency domain array processing provides the same steady-state MSE performance as that offered by the STAP system, using tapped delay-lines (TDL). Reference [17] provides important comparison results between the centralized and localized feedback schemes. However, such comparison was limited to the simulation results, and analytical support was not presented.

In this paper, we consider the analytical results of MSE performance of subband arrays with the three different feedback schemes. To the best of our knowledge, such results for the localized and partial feedback schemes have not yet been produced. It is shown in the following discussion that, unlike the centralized feedback subband array, which gives the optimum spatio-temporal equalization performance, the MSE performance provided by the localized and partial feedback subband arrays are generally suboptimal. The performance of these two suboptimal feedback schemes depends on the channel characteristics, the filter banks employed, and the number of subbands.

This paper is organized as follows. In Sect. 2, we introduce the signal model, and the steady-state MSE performance of the STAP systems is described. In Sect. 3, the subband decomposition is introduced, and the steady-state MSE performance of the centralized feedback subband array is derived and shown to be equivalent to the optimum STAP results. Section 4 analyzes the steady-state MSE performance of localized feedback subband arrays. In Sect. 5, the partial feedback scheme is proposed and its steady-state MSE performance is analyzed. Section 6 provides simulation examples for the covariance matrices of the original and the subband signals. The MSE results are compared for different feedback schemes.

2. Signal Model

We consider a base station that uses an antenna array of N sensors with P users, where $P < N$. The signal of interest is denoted by $s_1(l), l \in (-\infty, \infty)$, whereas the signals from the other users are denoted by $s_p(l)$, $p = 2, ..., P$. Accordingly, the received signal vector $\vec{x}(l)$ at the array, expressed in discrete form, is given by

$$\vec{x}(l) = \sum_{p=1}^{P} \sum_{m=-\infty}^{\infty} s_p(m)\vec{h}_p(l-m) + \vec{b}(l) \tag{1}$$

where

$s_p(l)$: information symbol of the pth user,

$\vec{h}_p(l)$: channel response vector of the pth user,

$\vec{b}(l)$: additive noise vector.

In this paper, we restrict the discussion to T-spaced equalization (i.e., sampled at the symbol rate) for simplicity. We make the following assumptions.

(A1) The user signals $s_p(l), p = 1, 2, ..., P$, are wide-sense stationary and independent and identically distributed (i.i.d.) with $E[s_p(l)s_p^*(l)] = 1$, where the superscript * denotes complex conjugate.

(A2) All channels $\vec{h}_p(l), p = 1, 2, ..., P$, are linear time-invariant and of a finite duration within $[0, D_p]$. That is, $\vec{h}_p(l) = 0, p = 1, 2, ..., P$, for $l > D_p$ and $l < 0$.

(A3) The noise vector $\vec{b}(l)$ is zero-mean, temporally and spatially white with

$$E[\vec{b}(l)\vec{b}^T(l)] = \mathbf{0}, \quad \text{and} \quad E[\vec{b}(l)\vec{b}^H(l)] = \sigma\mathbf{I}_N,$$

where the superscripts ^{T} and ^{H} denote transpose and conjugate transpose, respectively, σ is the noise power, and $\mathbf{I}_N$ is the $N \times N$ identity matrix.

Considering M successive snapshots, we have

$$\mathbf{x}(l) = \sum_{p=1}^{P} \mathbf{H}_p \mathbf{s}_p(l) + \mathbf{b}(l) \tag{2}$$

where

$$\mathbf{x}(l) = [\, \vec{x}^T(l) \ \vec{x}^T(l-1) \ \cdots \ \vec{x}^T(l-M+1)\,]^T \tag{3}$$

$$\mathbf{H}_p = \begin{bmatrix} \vec{h}_p(0) & \cdots & \vec{h}_p(D_p) & 0 & \cdots & \cdots & 0 \\ 0 & \vec{h}_p(0) & \cdots & \vec{h}_p(D_p) & 0 & \cdots & 0 \\ \vdots & & & & & & \vdots \\ 0 & \cdots & \cdots & 0 & \vec{h}_p(0) & \cdots & \vec{h}_p(D_p) \end{bmatrix} \tag{4}$$

$$\mathbf{s}_p(l) = [s_p(l) \ s_p(l-1) \cdots \ s_p(l-M-D_p+1)]^T \tag{5}$$

and

$$\mathbf{b}(l) = t[\vec{b}^T(l) \ \vec{b}^T(l-1) \ \cdots \vec{b}^T(l-M+1)]^T. \tag{6}$$

Denote $\vec{w}(m)$ as the weight vector of the STAP system corresponding to $\vec{x}(l-m)$, and define $\mathbf{w}(l) = \left[\vec{w}^T(l), \cdots, \vec{w}^T(l-M+1)\right]^T$. Then, the output of the STAP becomes

$$y(l) = \mathbf{w}^T(l)\mathbf{x}(l) = \sum_{m=0}^{M-1} \vec{w}^T(m)\vec{x}(l-m). \tag{7}$$

Using the minimum mean square error (MMSE) criterion,

$$\begin{aligned} &\min_{\mathbf{w}} E\left|y(l) - s_1(l-v)\right|^2 \\ &\quad = \min_{\mathbf{w}} E\left|\mathbf{w}^T\mathbf{x}(l) - s_1(l-v)\right|^2 \end{aligned} \tag{8}$$

where $0 \le v \le M + D_1 - 1$ is an appropriate time delay which minimizes the MSE [10], then the optimum weight vector is given by the Weiner-Hopf solution

$$\mathbf{w}_{opt} = \mathbf{R}^{-1}\mathbf{r} \tag{9}$$

where

$$\mathbf{R} = E[\mathbf{x}^*(l)\mathbf{x}^T(l)] \tag{10}$$

is the correlation matrix of $\mathbf{x}(l)$, and

$$\mathbf{r} = E[\mathbf{x}^*(l)s_1(l-v)] \tag{11}$$

is the cross-correlation vector between $\mathbf{x}(l)$ and the training signal, which is assumed to be an ideal replica of $s_1(l)$. The superscript * denotes complex conjugate. Substituting (2) to (11) yields

$$\begin{aligned}\mathbf{r} &= E\left[\left(\sum_{p=1}^{P}\mathbf{H}_p\mathbf{s}_p(l)+\mathbf{b}(l)\right)^* s_1(l-v)\right]\\ &= E\left[\mathbf{H}_1^*\mathbf{s}_1^*(l)s_1(l-v)\right] = \mathbf{H}_1^*\mathbf{e}_{v+1},\end{aligned} \tag{12}$$

where $\mathbf{e}_{v+1} = [0\ \cdots\ 0\ 1\ 0\cdots 0]^T$ is a vector whose elements are zero except that at the $v+1$ element being 1. It is obvious that $\mathbf{r}$ is the $(v+1)$-th column of $\mathbf{H}_1^*$.

Since $\mathbf{R}$ is Hermitian, then the MMSE is given by

$$\begin{aligned}\text{MMSE} &= E\left|\mathbf{w}_{opt}^T\mathbf{x}(l)-s_1(l)\right|^2\\ &= E\left|\mathbf{r}^T(\mathbf{R}^{-1})^T\mathbf{x}(l)-s_1(l)\right|^2\\ &= \mathbf{r}^T(\mathbf{R}^{-1})^T E[\mathbf{x}(l)\mathbf{x}^H(l)](\mathbf{R}^{-1})^*\mathbf{r}^*\\ &\quad - \mathbf{r}^T(\mathbf{R}^{-1})^T E[\mathbf{x}(l)s_1^*(l)]\\ &\quad + E[s_1(l)s_1^*(l)]\\ &\quad - \mathbf{r}^H\mathbf{R}^{-1}E[\mathbf{x}^*(l)s_1(l)]\\ &= 1-\mathbf{r}^H\mathbf{R}^{-1}\mathbf{r}.\end{aligned} \tag{13}$$

3. Subband Arrays

3.1 Subband Decomposition

Subband decomposition is performed by exploiting a set of analysis and synthesis filters. Discrete Fourier transform (DFT) and modified-QMF filter banks are examples of perfect reconstructed (PR) and near-perfect reconstruction (NPR) filter banks, respectively [8]. Decimation can be applied between the analysis filters and the synthesis filters to reduce the processing data rate. The decimation rate should not exceed the number of subbands. Such decimation, however, often reduces the steady state system performance due to aliasing. We maintain that, the PR and NPR properties can be easily destroyed if adaptive techniques are employed between the analysis filters and the synthesis filters because of the changes in the aliasing characteristics. In this paper, no decimation is performed for subband signal components. In this case, the synthesis filters are either not necessary, or can be integrated at the analysis filters.

Let the subband decomposition divide the data sequence at the output of ith virtual channel, $\tilde{x}_i(l)$, into Q subband sequences, $x_i^{(1)}(l),\cdots,x_i^{(Q)}(l)$, where the superscript (m) denotes the signal component at the mth subband. We define

$$\mathbf{x}_T(l) = \left[\left(\vec{x}_T^{(1)}(l)\right)^T,\cdots,\left(\vec{x}_T^{(Q)}(l)\right)^T\right]^T$$

as the signal vector for the subband arrays with

$$\vec{x}_T^{(m)}(l) = \left[x_1^{(m)}(l), x_2^{(m)}(l)\cdots, x_N^{(m)}(l)\right]^T.$$

As a general expression, we can relate $\mathbf{x}_T(l)$ and $\mathbf{x}(l)$ by a $QN\times MN$ transform matrix as

$$\mathbf{x}_T(l) = \mathbf{T}\mathbf{x}(l). \tag{14}$$

We only consider the specific cases where $\mathbf{T}$ is square (i.e., $Q=M$) and unitary (i.e., $\mathbf{T}\mathbf{T}^H = \mathbf{T}^H\mathbf{T} = \mathbf{I}_{MN}$). That is, the number of subbands is set equal to the number of the snapshots at each array sensor. This kind of subband processing is also known as real-time transform-domain processing [18].

A good example of such transform is the DFT filter bank, where the transform matrix $\mathbf{T}$ can be expressed in the form

$$\mathbf{T} = \mathbf{P}^T(\mathbf{I}_N\otimes\mathbf{T}_o)\mathbf{P} \tag{15}$$

where $\otimes$ denotes Kronecker product, and

$$\mathbf{T}_o = \frac{1}{\sqrt{M}}\cdot\begin{bmatrix} W_M^0 & W_M^0 & W_M^0 & \cdots & W_M^0\\ W_M^0 & W_M^1 & W_M^2 & \cdots & W_M^{M-1}\\ \vdots & & & & \vdots\\ W_M^0 & W_M^{M-1} & W_M^{2(M-1)} & \cdots & W_M^{(M-1)^2}\end{bmatrix} \tag{16}$$

with $W_M = \exp\left(\frac{-2\pi j}{M}\right)$. In (15), $\mathbf{P}$ is a permutation matrix to change the order of the elements of vector $\mathbf{x}(l)$ such that the M samples at each array sensor align together.

The DFT filter bank satisfies the PR condition [19] because the only non-zero sum of the column vectors (i.e., the coefficients of the analysis filters for different subbands) of $\mathbf{T}_o$ appears at the first column.

3.2 Subband Array with Centralized Feedback

In this part, we consider the subband array with centralized feedback scheme, as illustrated in Fig. 1. Weighting $\mathbf{x}_T(l)$ by the weight vector $\mathbf{w}_T = \left[(\mathbf{w}_T^{(1)})^T\ (\mathbf{w}_T^{(2)})^T\ \cdots\ (\mathbf{w}_T^{(M)})^T\right]^T$, the output of the transform domain array system becomes

$$y_T(l) = \mathbf{w}_T^T\mathbf{x}_T(l) = \mathbf{w}_T^T\mathbf{T}\mathbf{x}(l). \tag{17}$$

Again, using the MMSE creterion

$$\min_{\mathbf{w}_T} E\left|y_T(l)-s_1(l-v)\right|^2$$

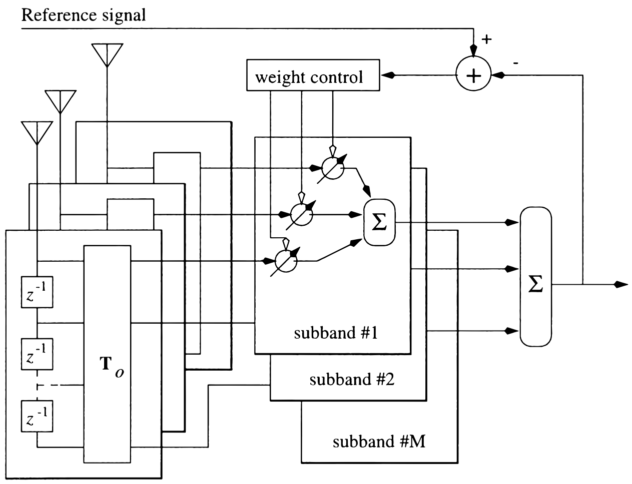

Fig. 1 Subband array with centralized feedback.

$$= \min_{\mathbf{w}_T} E\left|\mathbf{w}_T^T\mathbf{x}_T(l) - s_1(l-v)\right|^2, \tag{18}$$

the optimum weight vector becomes

$$\mathbf{w}_{T,opt} = \mathbf{R}_T^{-1}\mathbf{r}_T = (\mathbf{T}^T)^{-1}\mathbf{w}_{opt} \tag{19}$$

where

$$\mathbf{R}_T = E[\mathbf{x}_T^*(l)\mathbf{x}_T^T(l)] = \mathbf{T}^*\mathbf{R}\mathbf{T}^T \tag{20}$$

is the correlation matrix of $\mathbf{x}_T(l)$, and

$$\mathbf{r}_T = E[\mathbf{x}_T^*(l)s_1(l-v)] = \mathbf{T}^*\mathbf{r} \tag{21}$$

is the cross-correlation vector between $\mathbf{x}_T(l)$ and $s_1(l-v)$. When the optimum weight vectors are used for both STAP and the subband array, it is straightforward to show

$$y_T(l) = \mathbf{w}_{T,opt}^T\mathbf{T}\mathbf{x}(l) = \mathbf{w}_{opt}^T\mathbf{x}(l) = y(l), \tag{22}$$

and that the MSE of the subband array equals to the MMSE of the STAP systems

$$\begin{aligned}\mathrm{MSE}_{CF} &= E\left|y_T(l) - s_1(l-v)\right|^2 \\ &= E\left|y(l) - s_1(l-v)\right|^2 \\ &= \mathrm{MMSE}.\end{aligned} \tag{23}$$

4. Subband Array with Localized Feedback

4.1 Structure

Subband arrays with the localized feedback scheme are often used for reduced system complexity and improved convergence performance. The basic idea behind the localized feedback is that the signal correlation between signals at different subbands are often small due to the decorrelation function of the subband decomposition. Therefore, the signals at different subbands can be processed separately. A subband array with localized feedback scheme is illustrated in Fig. 2.

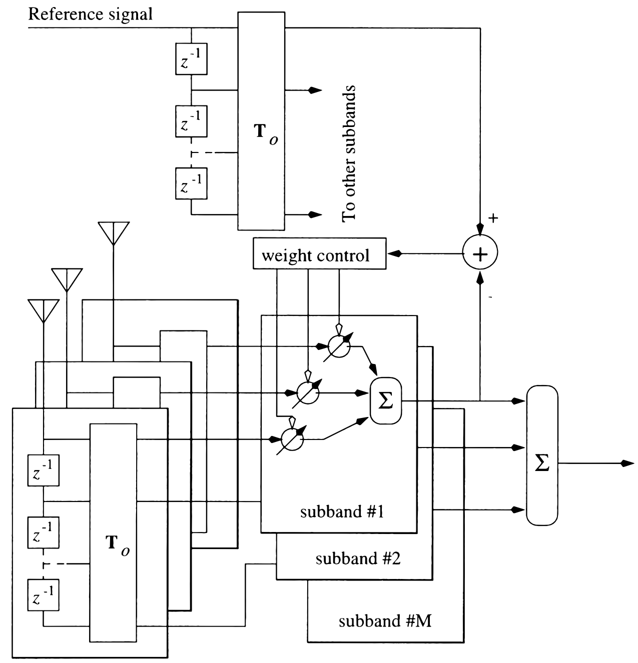

Fig. 2 Subband array with localized feedback.

In the localized feedback scheme, the reference signal is decomposed into its subband version

$$s_1^{(m)}(l-v) = \frac{1}{\sqrt{M}}\mathbf{T}_o^{(m)}\vec{s}_1(l-v), \tag{24}$$

which is then used as the reference signal at the mth subband, where

$$\mathbf{T}_o^{(m)} = \frac{1}{\sqrt{M}}[W_M^0 \; W_M^m \; \cdots \; W_M^{(M-1)m}] \tag{25}$$

is the mth row of the matrix $\mathbf{T}_o$, and

$$\begin{aligned}\vec{s}_1(l-v) &= [s_1(l-v) \; s_1(l-v-1) \\ &\qquad \cdots s_1(l-v-M+1)]^T\end{aligned}$$

is the M samples of the reference signal used for the subband decomposition. The factor $1/\sqrt{M}$ used in (24) is to normalize the power of the reference signal at each subband because

$$\begin{aligned}&\sum_{m=0}^{M-1}\mathbf{T}_o^{(m)}\vec{s}_1(l-v) \\ &\quad = \left[\sum_{m=0}^{M-1}W_M^0 \; \sum_{m=0}^{M-1}W_M^0 \cdots \sum_{m=0}^{M-1}W_M^0\right]\vec{s}_1(l-v) \\ &\quad = \sqrt{M}s_1(l-v).\end{aligned} \tag{26}$$

The $N \times 1$ weight vector at the mth subband, independent of other subbands, can be obtained from the $N \times N$ correlation matrix $\mathbf{R}_T^{(m)} = E\left[\mathbf{x}_T^{(m)}(l)(\mathbf{x}_T^{(m)}(l))^H\right]$ and the $N \times 1$ correlation vector $\mathbf{r}_T^{(m)} = E\left[\left(\mathbf{x}_T^{(m)}(l)\right)^* s_1^{(m)}(l-v)\right]$ as

$$\mathbf{w'}_T^{(m)} = (\mathbf{R}_T^{(m)})^{-1}\mathbf{r}_T^{(m)}. \tag{27}$$

4.2 Performance Analysis

Denote

$$\mathbf{R}'_T = \begin{bmatrix} \mathbf{R}_T^{(1)} & \mathbf{0} & \cdots & \mathbf{0} \\ \mathbf{0} & \mathbf{R}_T^{(2)} & \cdots & \mathbf{0} \\ \vdots & & & \vdots \\ \mathbf{0} & \mathbf{0} & \vdots & \mathbf{R}_T^{(M)} \end{bmatrix} \tag{28}$$

and

$$\mathbf{r}'_T = \left[\left(\mathbf{r}_T^{(1)}\right)^T \quad \left(\mathbf{r}_T^{(2)}\right)^T \quad \cdots \quad \left(\mathbf{r}_T^{(M)}\right)^T \right]^T. \tag{29}$$

Using the following property of block-diagonal matrix

$$(\mathbf{R}'_T)^{-1} = \begin{bmatrix} (\mathbf{R}_T^{(1)})^{-1} & \mathbf{0} & \cdots & \mathbf{0} \\ \mathbf{0} & (\mathbf{R}_T^{(2)})^{-1} & \cdots & \mathbf{0} \\ \vdots & & & \vdots \\ \mathbf{0} & \mathbf{0} & \vdots & (\mathbf{R}_T^{(M)})^{-1} \end{bmatrix}, \tag{30}$$

the weight vector of the localized feedback subband array can be expressed as

$$\mathbf{w}'_T = \begin{bmatrix} (\mathbf{R}_T^{(1)})^{-1}\mathbf{r}_T^{(1)} \\ (\mathbf{R}_T^{(2)})^{-1}\mathbf{r}_T^{(2)} \\ \vdots \\ (\mathbf{R}_T^{(M)})^{-1}\mathbf{r}_T^{(M)} \end{bmatrix} = (\mathbf{R}'_T)^{-1}\mathbf{r}'_T. \tag{31}$$

As implied from (28), $\mathbf{R}'_T$ is the block-diagonal approximation of $\mathbf{R}_T$ by ignoring its off-block-diagonal elements. On the other hand, the cross-correlation vector between the received signal vector and the reference signal at the mth subband is

$$\begin{aligned} \mathbf{r}_T^{(m)} &= E\left[\left(\mathbf{x}_T^{(m)}(l)\right)^* s_1^{(m)}(l-v)\right] \\ &= E\left[\left(\mathbf{T}^{(m)}\mathbf{x}(l)\right)^* s_1^{(m)}(l-v)\right] \\ &= E\left[\left(\mathbf{T}^{(m)}\right)^* \left(\sum_{p=1}^{P}\mathbf{H}_p\mathbf{s}_p(l)+\mathbf{b}(l)\right)^* \right. \\ &\qquad \left. \times \frac{1}{\sqrt{M}}\mathbf{T}_o^{(m)}\vec{s}_1(l-v)\right] \\ &= \frac{1}{\sqrt{M}}\left[\mathbf{T}^{(m)}\mathbf{H}_1\right]^* E\left[\mathbf{s}_1^*(l)\vec{s}_1^{\,T}(l-v)\right]\left[\mathbf{T}_o^{(m)}\right]^T \\ &= \frac{1}{\sqrt{M}}\left[\mathbf{T}^{(m)}\mathbf{H}_1\right]^* \mathbf{J}_v \left[\mathbf{T}_o^{(m)}\right]^T, \end{aligned} \tag{32}$$

where $\mathbf{T}^{(m)}$ is the $N \times MN$ submatrix of the matrix $\mathbf{T}$ corresponding to the mth subband, $\mathbf{J}_v$ is an $(M+D_1-1)\times M$ matrix expressed as, provided that we choose $v < D_1$,

$$\begin{aligned} \mathbf{J}_v &= E\left[\mathbf{s}_1^*(l)\vec{s}_1^{\,T}(l-v)\right] \\ &= [\mathbf{0}_v^T \quad \mathbf{I}_M \quad \mathbf{0}_{D_1-1-v}^T]^T, \end{aligned} \tag{33}$$

where $\mathbf{0}_v$ denotes the zero matrix of size $v \times M$.

Therefore, the MSE of the localized feedback subband array is given by

$$\begin{aligned} \mathrm{MSE}_{LF} &= E\left|s_1(l) - \mathbf{w}'^T_T\mathbf{x}_T(l)\right|^2 \\ &= 1 + \mathbf{r}'^H_T(\mathbf{R}'_T)^{-1}\mathbf{R}_T(\mathbf{R}'_T)^{-1}\mathbf{r}'_T \\ &\quad - 2\mathrm{Re}\left[\mathbf{r}'^H_T(\mathbf{R}'_T)^{-1}\mathbf{r}_T\right]. \end{aligned} \tag{34}$$

Equation (34) implies that the localized feedback subband array approach is suboptimal, and, its performance depends on the significance of the cross-correlation between signals at different subbands. It is clear from (20) and (34) that the off-block-diagonal elements of matrix $\mathbf{R}_T$ depends on both the transform matrix $\mathbf{T}$ and the channels $\mathbf{H}_p, p = 1, 2, ..., P$.

5. Partial Feedback Scheme of Subband Arrays

In the previous section, we discussed the subband array with the localized feedback scheme as an approximation of the subband array with the centralized feedback scheme. The former scheme has an independent weight update loop at each subband, at the cost of performance degradation, since the cross-correlations between different subbands are neglected in the weight estimation.

To provide more flexibility in trading-off the system performance and the complexity, we introduce subband arrays with the partial feedback scheme. As will be depicted, the partial feedback scheme is indeed a generalization of the centralized and localized feedback schemes, both can be considered as two extreme cases of the partial feedback scheme.

A subband array with partial feedback scheme is shown in Fig. 3, where the total M subbands are devided into K groups. The number of subbands in kth group is $M_k, k = 1, 2, ..., K$, with $M_1+M_2+\cdots+M_K = M$. In this paper, we consider the simple case of $M_1 = M_2 = \cdots = M_K = M/K$.

In this case, the signal covariance matrix $\mathbf{R}_T$ is approximated by a new block-diagonal matrix $\mathbf{R}''_T$ with a *larger* block size M_1N, expressed as

$$\mathbf{R}''_T = \begin{bmatrix} \mathbf{R}_T^{(G_1)} & \mathbf{0} & \cdots & \mathbf{0} \\ \mathbf{0} & \mathbf{R}_T^{(G_2)} & \cdots & \mathbf{0} \\ \vdots & & & \vdots \\ \mathbf{0} & \mathbf{0} & \vdots & \mathbf{R}_T^{(G_K)} \end{bmatrix} \tag{35}$$

where

$$\mathbf{R}_T^{(G_k)} = \begin{bmatrix} (\mathbf{R}_T)_{(k-1)M_1N+1,(k-1)M_1N+1} & \cdots \\ \vdots & \\ (\mathbf{R}_T)_{kM_1N,(k-1)M_1N+1} & \cdots \end{bmatrix}$$

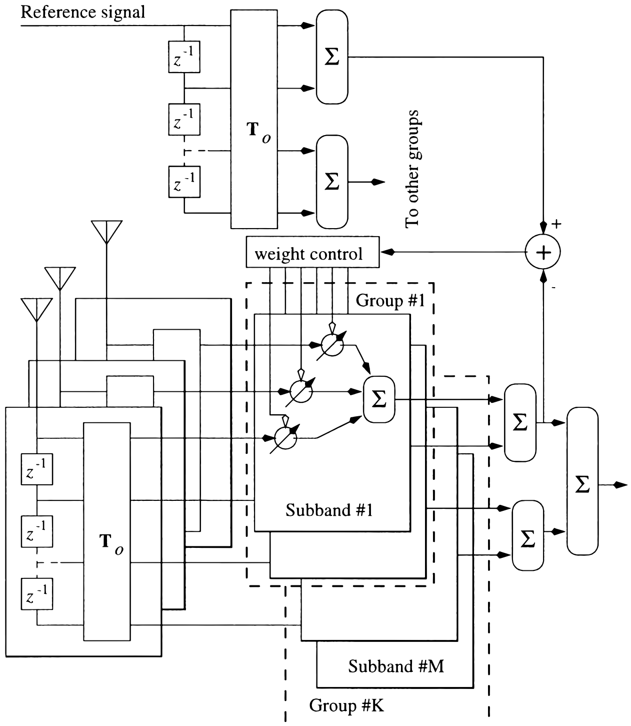

Fig. 3 Subband array with partial feedback.

$$\begin{matrix} \cdots & (\mathbf{R}_T)_{(k-1)M_1N+1,kM_1N} \\ & \vdots \\ \cdots & (\mathbf{R}_T)_{kM_1N,kM_1N} \end{matrix} \Bigg] \tag{36}$$

and $(\mathbf{R}_T)_{i,j}$ is the (i,j)-th element of matrix $\mathbf{R}_T$. When $M_1 > 1$, since fewer off-block-diagonal elements are ignored in $\mathbf{R}''_T$ as compared with $\mathbf{R}'_T$, the partial feedback scheme should provide more accurate optimum weights estimation and subsequently better MSE results than those of the localized feedback scheme.

Similar to (30), we have

$$(\mathbf{R}''_T)^{-1} = \begin{bmatrix} (\mathbf{R}_T^{(G_1)})^{-1} & \mathbf{0} & \cdots & \mathbf{0} \\ \mathbf{0} & (\mathbf{R}_T^{(G_2)})^{-1} & \cdots & \mathbf{0} \\ \vdots & & & \vdots \\ \mathbf{0} & \mathbf{0} & \vdots & (\mathbf{R}_T^{(G_K)})^{-1} \end{bmatrix}. \tag{37}$$

Therefore, the weight vector in the partial feedback scheme is given by

$$\mathbf{w}''_T = (\mathbf{R}''_T)^{-1}\mathbf{r}''_T = \begin{bmatrix} (\mathbf{R}_T^{(G_1)})^{-1}\mathbf{r}_T^{(G_1)} \\ (\mathbf{R}_T^{(G_2)})^{-1}\mathbf{r}_T^{(G_2)} \\ \vdots \\ (\mathbf{R}_T^{(G_K)})^{-1}\mathbf{r}_T^{(G_K)} \end{bmatrix} \tag{38}$$

where

$$\mathbf{r}_T^{(G_k)} = E\left[\left(\mathbf{x}_T^{(G_k)}(l)\right)^* s_1^{(G_k)}(l)\right], \tag{39}$$

Table 1 Parameters of the signal of user 1.

	h_1	AOA (deg)
$\tau = 0$	$0.7016 + j0.0000$	33.54
$\tau = T$	$0.1188 + j0.0570$	18.06
$\tau = 2T$	$-0.1353 + j0.3165$	38.26
$\tau = 3T$	$-0.2231 - j0.1808$	5.89
$\tau = 4T$	$0.1476 + j0.2898$	34.79
$\tau = 5T$	$-0.3106 - j0.2945$	30.78

Table 2 Parameters of the signal of user 2.

	h_2	AOA (deg)
$\tau = 0$	$0.6787 + j0.0000$	47.77
$\tau = T$	$0.1561 - j0.0592$	54.82
$\tau = 2T$	$-0.2173 + j0.3342$	68.07
$\tau = 3T$	$-0.2801 + j0.1987$	55.60
$\tau = 4T$	$-0.1119 + j0.2950$	39.89
$\tau = 5T$	$-0.3122 + j0.1938$	44.11

$$\mathbf{r}''_T = \left[\left(\mathbf{r}_T^{(G_1)}\right)^T \ \cdots \ \left(\mathbf{r}_T^{(G_K)}\right)^T\right]^T, \tag{40}$$

$s_1^{(G_k)}$ is the reference signal at the kth group, and

$$\mathbf{x}_T^{(G_k)}(l) = \left[\left(\mathbf{x}_T^{((k-1)M_1+1)}(l)\right)^T \ \cdots \ \left(\mathbf{x}_T^{(kM_1)}(l)\right)^T\right]^T. \tag{41}$$

The MSE of the partial feedback subband array is therefore

$$\begin{aligned} \mathrm{MSE}_{PF} &= E\left|s_1(l) - \mathbf{w}''^T_T\mathbf{x}_T(l)\right|^2 \\ &= 1 + \mathbf{r}''^H_T(\mathbf{R}''_T)^{-1}\mathbf{R}_T(\mathbf{R}''_T)^{-1}\mathbf{r}''_T \\ &\quad - 2\mathrm{Re}\left[\mathbf{r}''^H_T(\mathbf{R}''_T)^{-1}\mathbf{r}_T\right]. \end{aligned} \tag{42}$$

6. Simulation Results

A three-element linear array with half wavelength inter-element spacing is considered. Two user signals are illuminating the array (P=2), each has a maximum delay spread of 5 symbols ($D = D_1 = D_2 = 5$). Six multipaths are randomly generated for each user whose detailed parameters are given in Tables 1 and 2, respectively. The input signal-to-noise ratio (SNR) is 20 dB for both signals.

Figures 4(a) and (b) show the magnitude of the correlation matrices $\mathbf{R}$ and $\mathbf{R}_T$, where M=8. In Fig. 4(a), −60 dB is used to represent zero values so as to avoid errors in decibel calculation. In Figs. 5(a) and (b), we show similar results for M=32. It is clear that, while the value of $\mathbf{R}$ for different taps would be

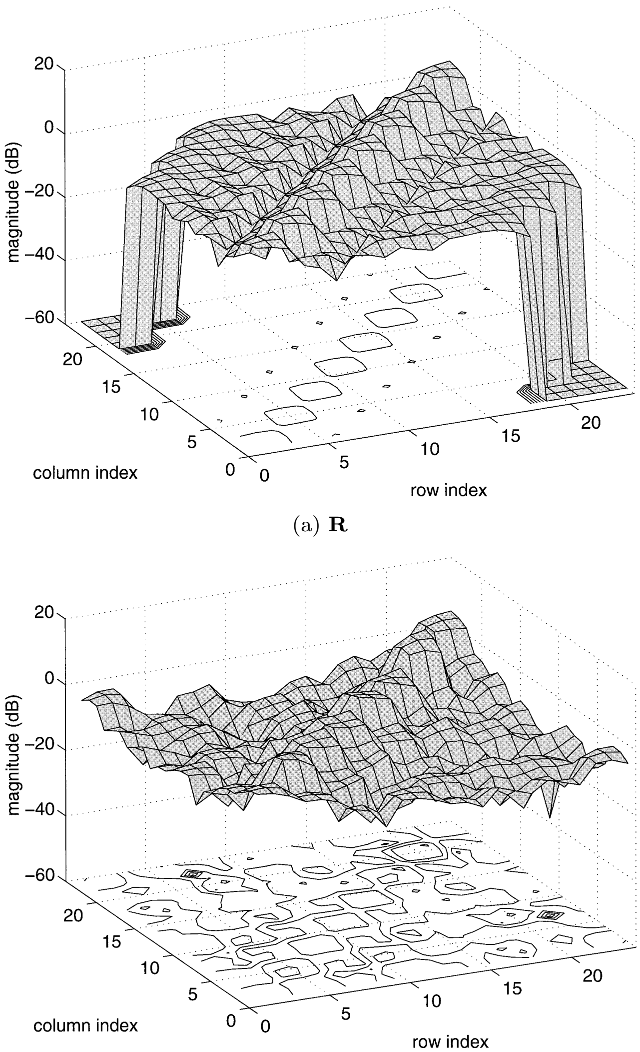

(a) $\mathbf{R}$

(b) $\mathbf{R}_T$

Fig. 4 Magnitudes of elements of $\mathbf{R}$ and $\mathbf{R}_T$ (M=8).

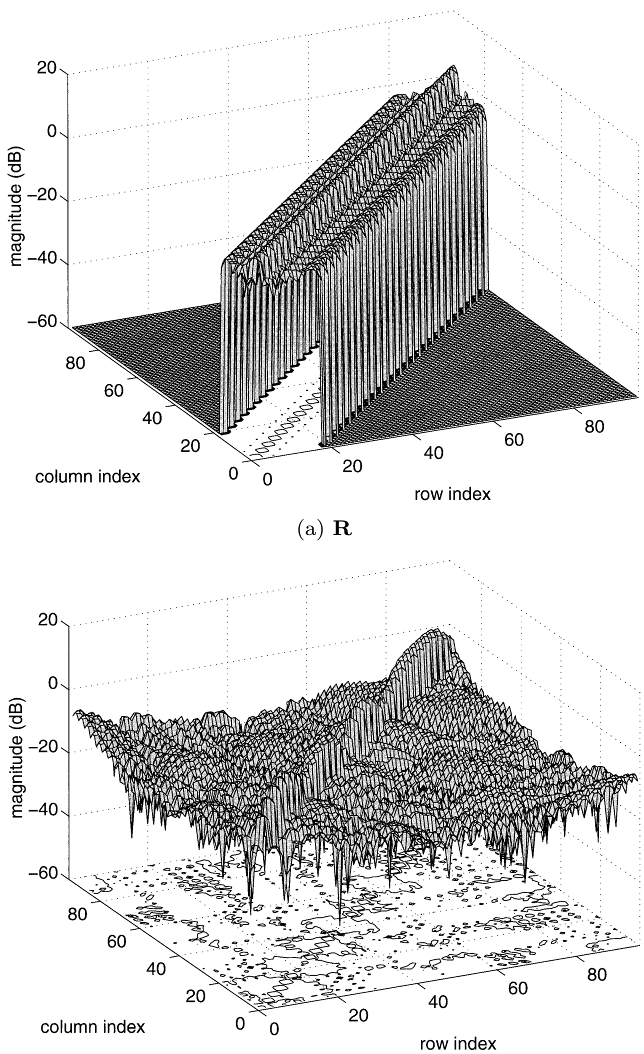

(a) $\mathbf{R}$

(b) $\mathbf{R}_T$

Fig. 5 Magnitudes of elements of $\mathbf{R}$ and $\mathbf{R}_T$ (M=32).

large depending on the channel coefficients, the value of $\mathbf{R}_T$ between different subbands becomes much smaller. However, the cost is increased floor values of the correlation matrix. The sidelobe effect is reduced as the number of subbands increases, as evident when comparing Fig. 4 and Fig. 5. This reduction is responsible for improving the MSE performance and pushing it closer to the optimum MMSE.

Figure 6 shows the MSE performance for different feedback schemes. The number of subbands M changes from 4 to 32, and the MSE performance at different values of M_1 are evaluated. The dashed line shows the asymptotical lower bound of the MSE as M increases towards infinity. It is shown in Fig. 6 that the difference between different feedback schemes is large when M is relatively small (M is 4 or 8 in this figure) and small for large value of M (M is 16 or 32). Therefore, the subband array with localized or partial feedback schemes

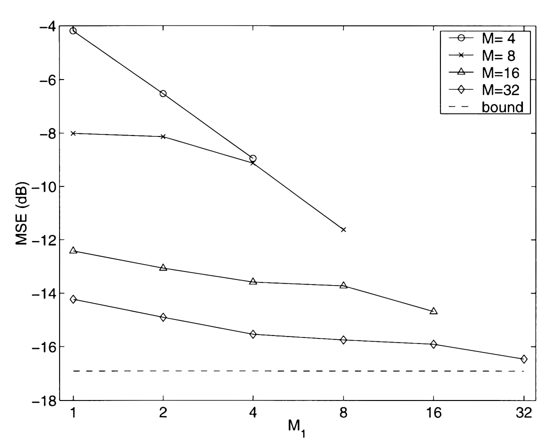

Fig. 6 MSE performance versus M and M_1.

can closely approach the optimum MMSE performance when increasing the number of subbands.

7. Conclusion

We have analyzed the performance of subband arrays with different types of feedback schemes, and the expressions of the steady-state mean square error (MSE) have been derived. It has been shown that subband arrays with localized and partial feedback schemes are generally suboptimal, and their performance depends on the channel characteristics, the filter banks employed, and the number of subbands. The proposed partial feedback scheme generalizes the subband arrays with centralized and localized feedback schemes, and provides more flexibility in trading-off the system complexity with the MSE performance.

Acknowledgment

Y. Zhang and K. Yang would like to thank Dr. B. Komiyama and Dr. T. Ohira, ATR Adaptive Communications Research Laboratories, Japan, for their encouragement and helpful discussions. Y. Zhang also thanks the valuable discussions by Prof. W. Wong and Prof. Z. Luo, McMaster University, Canada.

References

[1] Y. Ogawa, M. Ohmiya, and K. Itoh, "An LMS adaptive array for multipath fading reduction," IEEE Trans. Aerosp. & Electron. Syst., vol.AES-23, no.1, pp.17–23, Jan. 1987.
[2] R. Kohno, "Spatial and temporal communication theory using adaptive antenna array," IEEE Personal Communications, vol.5, no.1, pp.28–35, Feb. 1998.
[3] Y. Doi, T. Ohgane, and E. Ogawa, "ISI and CCI canceller combining the adaptive array antennas and the Viterbi equalizer in a digital mobile radio," Proc. IEEE VTC, pp.81–85, April 1996.
[4] A.J. Paulraj and C.B. Papadias, "Space-time processing for wireless communications," IEEE Signal Processing Magazine, vol.14, no.6, pp.49–83, Nov. 1997.
[5] Y. Zhang, K. Yang, and M.G. Amin, "Adaptive subband arrays for multipath fading mitigation," Proc. IEEE Antennas & Propag. Society Int. Symp., pp.380–383, Atlanta, GA, June 1998.
[6] Y. Zhang, K. Yang, and M.G. Amin, "Performance analysis of subband adaptive arrays in multipath propagation environment," Proc. IEEE Signal Processing Workshop on Statistical Signal and Array Processing, pp.17–20, Portland, OR, Sept. 1998.
[7] Y. Zhang, K. Yang, and Y. Karasawa, "Subband CMA adaptive arrays in multipath fading environment," IEICE Trans., vol.J82-B, no.1, pp.97–108, Jan. 1999.
[8] Y. Zhang, K. Yang, and M.G. Amin, "Adaptive array processing for multipath fading mitigation via exploitation of filter banks," IEEE Trans. Antennas & Propag., vol.49, no.4, pp.505–516, April 2001.
[9] K. Yang, Y. Zhang, and Y. Mizuguchi, "Subband realization of space-time adaptive processing for mobile communications," Proc. Int. Symp. on Personal, Indoor and Mobile Radio Communications, no.D2-3, Osaka, Sept. 1999.
[10] K. Yang, Y. Zhang, and Y. Mizuguchi, "A signal subspace-based approach to space-time adaptive processing for mobile communications," IEEE Trans. Signal Processing, vol.49, no.2, pp.401–413, Feb. 2001.
[11] J.M. Khalab and M.K. Ibrahim, "Novel multirate adaptive beamforming technique," Electron. Lett., vol.30. no.15, pp.1194–1195, 1994.
[12] Y. Zhang, K. Yang, and M.G. Amin, "Convergence performance of subband arrays for spatio-temporal equalization," Proc. IEEE Statistical Signal Processing Workshop, Singapore, Aug. 2001.
[13] T. Sekiguchi and Y. Karasawa, "CMA adaptive array antennas using analysis and synthesis filter banks," IEICE Trans. Fundamentals, vol.E81-A, no.8, pp.1570–1577, Aug. 1998.
[14] H. Hoffman and S. Kogon, "Subband STAP in wideband radar systems," Proc. IEEE Sensor Array and Multichannel Signal Processing Workshop, pp.256–260, Cambridge, MA, March 2000.
[15] A. Steinhardt, "Subband STAP processing: The fifth generation," Proc. IEEE Sensor Array and Multichannel Signal Processing Workshop, pp.1–6, Cambridge, MA, March 2000.
[16] R.T. Compton, "The relationship between tapped delay-line and FFT processing in adaptive arrays," IEEE Trans. Antennas & Propag., vol.36, no.1, pp.15–26, Jan. 1988.
[17] Y. Kamiya and Y. Karasawa, "Performance comparison and improvement in adaptive arrays based on time and frequency domain signal processing," IEICE Trans., vol.J82-A, no.6, pp.867–874, June 1999.
[18] F. Beaufays, "Transform-domain adaptive filters: An analytical approach," IEEE Trans. Signal Processing, vol.43, no.2, pp.422–431, Feb. 1995.
[19] G. Strang and T. Nguyen, Wavelets and Filter Banks, Wellesley-Cambridge Press, Wellesley, MA, 1996.

Yimin Zhang received his M.Sc. and Ph.D. degrees from the University of Tsukuba, Japan, in 1985 and 1988, respectively. He joined the Southeast University, Nanjing, China, in 1988. He served as a Senior Technical Manager at Communication Laboratory Japan, Kawasaki, Japan, from 1995 to 1997, and a Visiting Researcher at ATR Adaptive Communications Research Laboratories, Kyoto, Japan, from 1997 to 1998. Currently, he is a Post-Doctoral Research Associate at the Villanova University. His current research interests are in the areas of array signal processing, space-time adaptive processing, multiuser detection, blind signal processing, digital mobile communications, and time-frequency analysis. Dr. Zhang is a member of IEEE.

Kehu Yang received the B.E., M.S., and Ph.D. degrees from Xidian University (formerly the Northwest Telecommunication Engineering Institute), Xi'an, China, in 1982, 1984, and 1995, respectively. Dr. Yang joined Xidian University in 1985, where he became an Associate Professor in 1996. Since December 1998, he has been a visiting researcher at ATR Adaptive Communications Research Laboratories, Kyoto, Japan. His research interests include space-time adaptive processing for mobile communications, array signal processing. Dr. Yang is a member of IEEE.

Moeness G. Amin received the Ph.D. degree in electrical engineering in 1984 from the University of Colorado, Boulder. He has been on the Faculty of the Department of Electrical and Computer Engineering, Villanova University, Villanova, PA, since 1985, where is now a Professor. His current research interests are in the areas of time-frequency analysis, spread spectrum communications, smart antennas, and blind signal processing. Dr. Amin was an Associate Editor of the IEEE Transactions on Signal Processing and is currently a member of the IEEE Signal Processing Society Technical Committee on Signal Processing for Communications. He was the General Chair of the 1994 IEEE International Symposium on Time-Frequency and Time-Scale Analysis and the General Chair of the 2000 IEEE Workshop on Statistical Signal and Array Processing. He is the recipient of the 1997 IEEE Philadelphia Section Award and the IEEE Third Millennium Medal. He serves on the Committee of Science and Arts of the Franklin Institute. Dr. Amin is a Fellow of IEEE.

Yoshio Karasawa received the B.E. degree from Yamanashi University in 1973, and the M.S. and Dr.Eng. degrees from Kyoto University in 1977 and 1992, respectively. He joined KDD R&D Labs. in 1977. From July 1993 to July 1997, he was a Department Head of ATR Optical and Radio Communications Res. Labs., and ATR Adaptive Communications Res. Labs., both in Kyoto. From 1997 to 1999, he was a Senior Project Manager of KDD R&D Labs. Now he is a Professor at the University of Electro-Communications, Tokyo. Since 1977, he has been engaged in studies on wave propagation and radio communication antennas, particularly on theoretical analysis and measurements for wave propagation phenomena, such as multipath fading in mobile radio systems, tropospheric and ionospheric scintillation, and rain attenuation. His recent interests are in study on the frontier region bridging "wave propagation" and "digital transmission characteristics" in wideband mobile-radio systems, and digital and optical signal processing antennas. Dr. Karasawa received the Young Engineers Award from the IECE of Japan in 1983, and the Meritorious Award on Radio from the Association of Radio Industries and Businesses (ARIB, Japan) in 1998. He is a member of the IEEE.